01 Aug 2002

Anticipating Full Vehicle Radiated EMI from Module-Level Testing in Automobiles

Geping Liu

Chingchi Chen

Yuhua Tu

James L. Drewniak
Missouri University of Science and Technology, drewniak@mst.edu

Recommended Citation

G. Liu et al., "Anticipating Full Vehicle Radiated EMI from Module-Level Testing in Automobiles," *Proceedings of the IEEE International Symposium on Electromagnetic Compatibility (2002, Minneapolis, MN)*, vol. 2, pp. 982-986, Institute of Electrical and Electronics Engineers (IEEE), Aug 2002.
The definitive version is available at https://doi.org/10.1109/ISEMC.2002.1032829

Anticipating Full Vehicle Radiated EMI from Module-Level Testing in Automobiles

Geping Liu
EMC Lab, ECE Dept.
Univ. of Missouri-Rolla
Rolla, MO, U.S.A.
geping@umr.edu

Chingchi Chen
Ford Research Lab
Ford Motor
Dearborn, MI, U.S.A.
cchen4@ford.com

Yuhua Tu and James L. Drewniak
EMC Lab, ECE Dept.
Univ. of Missouri-Rolla
Rolla, MO, U.S.A.
drewniak@ece.umr.edu

Abstract
EMI due to common-mode currents on cables routed in automobiles was studied using a test device designed to mimic a vehicle. Both experimental work and Finite-Difference Time-Domain (FDTD) modeling were employed in this paper. The good agreement between the measurements and modeling results indicates that the numerical tools can be a useful aid in predicting vehicle-level EMI by developing vehicle transfer functions and measuring the module-level EMI characteristics on the bench top.

Keywords
Transfer function, FDTD, EMI and common-mode current

INTRODUCTION

Commercial vehicles need to satisfy stringent EMC criteria to prevent interference in nearby electronic systems. Many studies show that a switching power electronics module can be a dominant noise source, which results in the common-mode currents on the cables located in the vehicle. The EMI in the frequency range of 10 kHz —1000 MHz is a primary concern in automotive applications, and module-level EMI specifications are carefully followed during early development stages. However, due to system complexity, vehicle-level EMC performance is still not guaranteed. Nevertheless, complicated vehicle-level issues can be reduced to simpler module-level matters, and some potential EMC problems can be discovered in early development stages.

Paul emphasized the need to consider and model common-mode currents in order to adequately predict radiation from printed circuit boards [4], [5]. Simple equations are available in [6] to estimate the radiation from conducted emissions. However, these formulations are only appropriate for very simple geometries and at lower frequencies / shorter cables where current distributions are roughly uniform. Hockanson et. al. described two fundamental EMI source mechanisms resulting in common-mode current on a cable attached to a PCB and demonstrated the utility of FDTD modeling for common-mode radiation analysis [7], [8]. The coupling between high-speed digital and I/O lines is studied in a multi-stage modeling fashion in [9]. Empirical transfer functions based on current and field measurements in an anechoic chamber are used with laboratory (non-anechoic chamber) measured common-mode current data for radiated emissions prediction in [10]. Chen proposed simple efficient empirical strategies to predict system-level emission from the known subsystem-level characteristics [3].

This paper proposes an effective strategy to characterize the transfer function for anticipating full vehicle-level EMI. Using the full vehicle-level transfer function determined from FDTD modeling of the vehicle environment, automotive engineers can predict full vehicle-level emissions from known module-level characteristics during the design cycle of the electronic module. Section 1 describes the detailed characterization procedure of predicting the full-vehicle level radiation. Section 2 presents the relevant measurement techniques and FDTD modeling approach that are utilized in the characterization procedure. Results from the procedure and direct measurements are then given.

1. TRANSFER FUNCTION CHARACTERIZATION PROCEDURE

The primary assumption made in the proposed approach is that the dominant radiated field component is due to common-mode currents on the cables. In a real vehicle, the electronic module, which is the source of the electrical noise, is too complicated to model, and the common-mode current on the cable cannot be calculated using FDTD modeling. However, measurement results and numerical modeling can be combined to predict full vehicle-level EMI. Full vehicle-level EMI can be anticipated from module-level measurements and knowledge of the vehicle-level transfer function. The vehicle-level transfer function is defined as the ratio of the radiated emission from the vehicle to the common-mode current on the cable at the feed point.

$$H(f) = \frac{|V_{ant}|}{|I_{cm}|} = \frac{|E|}{|I_{cm}|}\,|AF|, \qquad (1)$$

where V_{ant} is the voltage received at the terminals of the antenna, I_{cm} is the common-mode current on the cable, E is the electric field at the location of the antenna, and AF is the antenna factor of the antenna..

The procedure for estimating the full vehicl-level EMI is :

Step 1: Utilize a dual-current probe technique to measure the common-mode source impedance (Z_{cm}) looking into the power electronic module and an equivalent input imped-

0-7803-7264-6/02/$17.00 © 2002 IEEE

ance (Z_{in}) of the transmission line at the output terminals of the module on a conductive bench top [2].

Step 2: Model the specific cable routing, the vehicle geometry and other important details in FDTD method, thereby obtaining the full vehicle-level transfer function.

Step 3: Measure the common-mode current from the module-level testing on the bench top using a current probe.

Step 4: Calculate the full-vehicle level emissions from

$$|E| = |V_{ant}|/|AF| = |H(f)||I_{cm}|/|AF|, \quad (2)$$

where V_{ant} is the voltage at the receiving antenna terminals, AF is the antenna factor of the monopole antenna, $H(f)$ is the transfer function calculated from FDTD results, and I_{cm} is the common-mode current measured from the module-level testing setup.

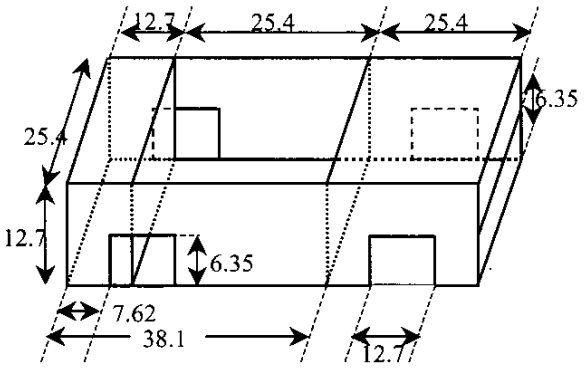

Figure 1. The geometry of the car model (units cm).

2. MEASUREMENT CONFIGURATION AND FDTD MODELING

2.1 Full vehicle-level measurement configuration and FDTD modeling

A scaled test device designed to approximate a portion of a real vehicle was constructed and the geometry is shown in Figure 1. The model was made of sheet aluminum. A 0.165-cm diameter wire was routed below the bottom of the model with a spacing of 1 cm as shown in Figure 2. One end of the wire was terminated on the center of the front firewall with a 150 Ω resistor soldered to a conductive adhesive copper tape square. The source was fed from Port 1 by a 0.085" semi-rigid coaxial cable with an SMA connector, which mimicked the common-mode noise source inside the power electronic enclosure. The outer shield of the cable was soldered to the bottom of the model at the feed point. The center conductor of the cable was extended and soldered to the wire routed along the bottom of the model. Port 2 of the network analyzer was connected to a 7.8-cm long receiving monopole-antenna. The monopole antenna was 10.4 cm away from the model, and 32 cm away from the left side of the model. The full vehicle-level system transfer function is defined from Equation (1).

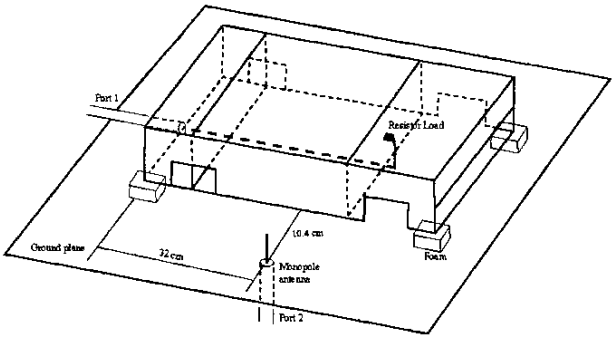

Figure 2. Full vehicle-level emission measurement setup.

The Finite-Difference Time-Domain (FDTD) method was employed to model the test configuration described in Figure 2. The FDTD cell size was 0.2 cm × 0.2 cm × 0.2 cm. All the aluminum plates were modeled as perfect electrical conductors (PEC) by enforcing the tangential electric field to be zero on the plates. The source cell was modeled as a 50 Ω impedance voltage source at the feeding point where the SMA jack was placed. The source function was a sinusoidally modulated Gaussian pulse. The receiving monopole antenna was modeled as a 7.62-cm long solid wire conductor with a thin wire algorithm [11], which was terminated on the ground with a 50 Ω resistor. The ground plane was modeled as an infinite PEC surface. Perfectly matched layer (PML) absorbing boundary conditions were used to limit the computational domain [12]. The current at the source cell and the voltage at the 50 Ω termination connected to the antenna were recorded, and the full vehicle-level system transfer function in the frequency domain was calculated using the Fast Fourier Transform (FFT) of the corresponding current and voltage time-histories.

For verification of the numerical results, a direct experimental method for obtaining the transfer function defined in Equation (1) was used. Port 1 of a network analyzer was connected to the SMA jack. Port 2 of the network analyzer was connected to the receiving monopole antenna. The scattering matrix parameter $|S_{21}|$ measured with the network analyzer can be expressed as

$$\left|S_{21}^{direct}\right| = \frac{\left|V_2^-\right|}{\left|V_1^+\right|} = \frac{|V_{ant}|}{|V_1|}|1+S_{11}| = \frac{|V_{ant}|}{|I_{cm}|}\frac{|1+S_{11}|}{|Z_{in}|}$$

$$= \frac{|V_{ant}|}{|I_{cm}|}\frac{|1+S_{11}|}{50\dfrac{|1+S_{11}|}{|1-S_{11}|}} = \frac{|V_{ant}|}{|I_{cm}|}\frac{|1-S_{11}|}{50} \quad (3)$$

where Z_{in} is an equivalent input impedance at the feeding point looking towards the transmission line. From Equation (2) and Equation (3), the transfer function is obtained as

$$H(f) = 50\frac{\left|S_{21}^{direct}\right|}{\left|1 - S_{11}\right|} \qquad (4)$$

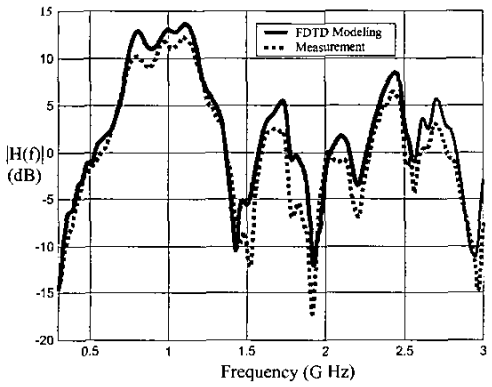

Figure 3. The full vehicle-level transfer function comparison between the FDTD modeling and direct measurements.

The modeling result and the measurement results are compared in Figure 3. In general, the FDTD modelled transfer function agrees well with the transfer function obtained from direct measurements.

2.2 Module-level measurement configuration

In the four-step full vehicle-level EMI characterization procedure, measurement techniques are critical to determine common-mode impedances and common-mode currents. A measurement setup was designed to represent a power electronic module on a conductive bench top. A transmission line was built by placing a 50 cm long wire 4.9 cm above a large aluminum plate as shown in Figure 4. The wire was terminated with a 270 Ω resistor at one end, which represented the module-level common-mode load resistance. The other end of the wire was soldered to the center conductor of an SMA jack terminated in 50 Ω resistor. The termination represented the module-level common-mode source impedance of the electronic module. A non-invasive measurement procedure with two current probes (Dual Current Probe Technique) was utilized herein to characterize the system impedance without disconnecting the cables [2].

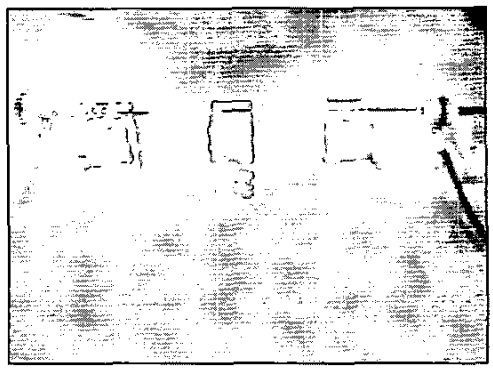

Figure 4. Module-level EMI characteristics measurement setup.

To measure the common-mode current from the electronic module on the bench top, the SMA jack was connected to Port 1 of a network analyzer, which mimicked the voltage-driven common-mode source inside the power electronic enclosure. A current probe connected to Port 2 of the network analyzer was clamped on the wire close to the SMA jack to measure the common-mode current. As shown in Figure 4, I_{cm}^{mod} is a common-mode current from the electronic module, V_{noise} is a voltage-driven common-mode source inside the module, $Z_{cm,s}$ is a common-mode source impedance of the module and Z_{in}^{mod} is an equivalent input impedance of the transmission line at the output terminals of the enclosure. The impedances $Z_{cm,s}$ and Z_{in}^{mod} can be measured and characterized by the Dual Current Probe Technique. Thus, the relation between the V_{noise} and I_{cm}^{mod} can be expressed as

$$I_{cm}^{\text{mod}} = \frac{V_{noise}}{Z_{cm,s} + Z_{in}^{\text{mod}}}. \qquad (5)$$

Meanwhile, the measured S_{21} result can be expressed as

$$S_{21}^{\text{mod}} = \frac{V_2^-}{V_1^+} = \frac{I_{cm}^{\text{mod}} Z_T}{V_1^+}, \qquad (6)$$

where Z_T is the transfer impedance of the current probe and V_1^+ is the incident voltage at Port 1 of the network analyzer.

The assumption is that the electronic module on the bench top has the same common-mode voltage-driven noise source and common-mode source impedance as those in the full vehicle. Since the Dual Current Probe Technique can be used to measure the equivalent input impedance of the cable at the output terminals of the enclosure in the vehicle, the common-mode current on the cable in the vehicle can be obtained as

$$I_{cm}^{veh} = \frac{V_{noise}}{Z_{cm,s} + Z_{in}^{veh}}. \qquad (7)$$

From Equation (5) and Equation (7), the common-mode current I_{cm}^{veh} is calculated from the known module-level EMI characteristics

$$I_{cm}^{veh} = I_{cm}^{\mathrm{mod}} \frac{Z_{cm,s} + Z_{in}^{\mathrm{mod}}}{Z_{cm,s} + Z_{in}^{veh}} . \qquad (8)$$

2.3 Prediction and measurement of full vehicle-level emissions

With the known full vehicle-level transfer function from FDTD modeling and the common-mode current from module-level measurements, the full vehicle-level emissions can be calculated. For convenience, the voltage received by the receiving monopole antenna was utilized herein to quantify the magnitude of the radiated electric field. Then,

$$|V_{ant}| = |E||AF| = |H(f)||I_{cm}^{veh}| = |H(f)||I_{cm}^{\mathrm{mod}}| \left| \frac{Z_{cm,s} + Z_{in}^{\mathrm{mod}}}{Z_{cm,s} + Z_{in}^{veh}} \right| , \qquad (9)$$

where AF, $H(f)$, I_{cm}^{veh}, I_{cm}^{mod}, $Z_{cm,s}$, Z_{in}^{mod}, Z_{in}^{veh} were as defined above. Substituting Equation (6) into Equation (9), the full vehicle-level emission is

$$|V_{ant}| = |H(f)| \frac{|S_{21}^{\mathrm{mod}}|}{|Z_T|} \left| \frac{Z_{cm,s}^{\mathrm{mod}} + Z_{in}^{\mathrm{mod}}}{Z_{cm,s}^{veh} + Z_{in}^{veh}} \right| |V_1^+| . \qquad (10)$$

To facilitate comparison of the full vehicle-level emissions from the characterization procedure with that from an independent direct measurement, a test setup was configured as shown in Figure 1. The SMA jack was connected to Port 1 of a network analyzer, which mimicked the voltage-driven common-mode source inside the power electronic enclosure. Port 2 was connected to the receiving monopole antenna. The directly measured full vehicle-level EMI can be simply expressed in terms of the S_{21} measurement result as

$$|V_{ant}^{dir}| = |V_2^-| = |S_{21}^{dir}||V_1^+| . \qquad (11)$$

The emission results from the characterization procedure, assuming $|V_1^+| = 1$, and the direct measurement are shown in Figure 5. The two results agree closely in the frequency range from 300 MHz to 3 GHz. The peaks of the results occur near the resonance frequencies of the transmission line in the vehicle, and the resonance frequencies of the receiving monopole antenna. The discrepancy between the two curves is due to a number of factors. Primarily, there are artifacts because of the influence of the current probe during the measurement procedure, especially at high frequencies. Second, the combination of the modeling and measurement results may contain calculation errors.

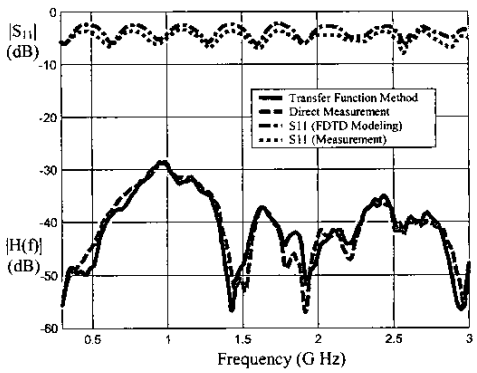

Figure 5. Full vehicle-level emission comparison between the EMI characterization procedure and the direct measurement (resistive load 150 Ω).

3. CONCLUSION AND DISCUSSION

The four-step EMI characterization procedure has been utilized to predict the full vehicle-level emission from both the FDTD modeling and module-level measurement results. Comparison of this approach with direct measurements supports its effective usage in anticipating EMI associated with common-mode source inside the electronic module in the vehicle. There are several advantages of the proposed approach. First, engineers can predict the complicated full vehicle-level EMC performance and discover the hidden EMC problems during the early development stages of the electronic module development. Another advantage is that the approach is non-invasive measurement approach and eliminates the need for a full-wave modeling in the whole characterization procedure.

The success of the study was based upon the assumption, that the dominant contributor to the radiated emissions was the common-mode current from the electronic module. In addition, the geometry of the vehicle and layout of the cable in the vehicle have a significant impact in the current measurements and radiation calculations. However the proposed method is still valid for a modified test setup.

Although this approach was originally proposed for the automotive industry, the hybrid FDTD modeling and measurement characterization method is also suitable for solving EMC problems in other applications. The approach allows reducing these complicated system-level issues to simpler subsystem-level matters for better prediction. The transfer function of a complex system can be calculated from other full-wave approaches, such as FEM modeling. Other measurement techniques, including the Dual Current Probe Technique, can be used in this hybrid method to obtain the subsystem EMC characteristics.

REFERENCES

[1] Timothy T. Pak, "EMI Investigation of A Hybrid Electric Vehicle Traction Drive", M.S. thesis, University of Missouri-Rolla, Rolla, M.O., U.S., Nov, 2000

[2] Yimin Ding, "Dual Current Probe Techniques for EMI Diagnosis and Characterization", M.S. thesis, University of Missouri-Rolla, Rolla, M.O., U.S., Aug 2000.

[3] C. Chen, "Predicting Vehicle-Level Radiated EMI Emission Using Module-Level Conducted EMIs and Harness Radiation Efficiencies", IEEE Int. Symp. Electromagn. Compat.,Montreal, Canada, 2001, pp1146-pp1151.

[4] C. R. Paul and D.R. Bush, "Radiated emission from common-mode currents", in Proc. 1987 IEEE Int. Symp. Electromag. Compat., Altanta, GA, Sept. 1987, IEEE Electromag. Compat. Soc., pp. 197-203.

[5] C. R. Paul, "A Comparison of the contributions of common-mode and differential-mode currents in radiated emissions", IEEE Transaction on Electromagnetic Compatibility, vol.31, pp. 189-193, May 1989.

[6] C.R. Paul, Introduction to Electromagnetic Compatibility, John Wiley & Sons, New York, 1992.

[7] D.M. Hockanson, J. L. Drewniak, T.H. Hubing, T.P. Van Doren, "FDTD modeling of common-mode radiation from cables", IEEE Transaction on Electromagnetic Compatibility, vol.38, no.3, pp. 376-387, August 1996.

[8] D.M. Hockanson, J. L. Drewniak, T.H. Hubing, T.P. Van Doren, "Investigation of fundamental EMI source mechanisms driving common-mode radiation from printed circuit boards with attached cables", IEEE Transaction on Electromagnetic Compatibility, vol.38, no.4, pp. 557-566, November 1996.

[9] W. Cui, M. Li, X. Luo, J.L. Drewniak, T.H. Hubing, T.P. Van Doren, R.E. DuBroff, "Anticipating EMI from coupling between high-speed digital and I/O lines", IEEE Int. Symp. Electromagn. Compat.,vol 1, 1999.

[10] W.T. Smith and R.K. Frazier, "Prediction of anechoic chamber radiated emissions measurements through use of empirically-derived transfer functions and laboratory common-mode current measurements", IEEE Int. Symp. Electromagn. Compat., 1998.

[11] A. Taflove, Computational Electrodynamics: The Finite-Difference Time-Domain Method, Norwood, MA: Artech House, Inc., 1995

[12] J.P. Berenger, "A perfectly matched layer for the absorption of electromagnetic waves", Journal of Computational Physics, vol. 114, no. 2, pp. 185-200, October 1994.